Chapter 4

CATALYTIC N_2-TO-NH_3 CONVERSION BY FE AT LOWER DRIVING FORCE: A PROPOSED ROLE FOR METALLOCENE-MEDIATED PCET

Reproduced in part with permission from:

Chalkley, M.; Del Castillo, T.; Matson, B.; Roddy, J.; Peters, J. C.; *ACS Central Science*, **2017**, 3, 217-223. **DOI:** 10.1021/acscentsci.7b00014

This was one of my favorite projects that I worked on at Caltech and there are actually two potentially valuable lessons to take away from it. The first is that one should generally follow one's advisor's advice (at least eventually), not only will this streamline future conversations with one's advisor, but also, occasionally, the ideas will even be worth pursuing on their own merit. Prior to this project the idea of finding a new combination of acid and reductant that would work with the P_3^BFe *catalyst to drive* N_2RR *had been kicked around the lab as a target essentially as long as I was with the group and no one had taken it up. Finally, Jonas had a small group of my colleagues and I assembled in his office and he said something to the effect of "I want this done, who's willing to do it?" I was in between interesting leads at the time so I raised my hand. The following research ended up being perhaps the most fruitful of my graduate career and ultimately unlocked my long-held dream of observing electrocatalytic* N_2RR *with the* P_3^BFe *catalyst. The other take away is about not being afraid to jump to conclusions; even if the reason for the conclusion is wrong it might still be a good idea. When I first got the data that decamethylcobaltocene could serve as a chemical* *reductant for N_2RR with the P_3^BFe catalyst we thought that this reaction must not be going through the anionic $P_3^BFeN_2^-$ state. The reason we thought this was because we didn't know the potential of the $P_3^BFeN_2^{0/-}$ couple under the relevant conditions and thought decamethylcobaltocene wouldn't be sufficiently reducing to access $P_3^BFeN_2^-$. That thinking turned out to be wrong, but for a time we had a new paradigm that went against our previous hypothesis that this reduced state was critical for N_2RR. That was the line of thinking that got us talking about PCET. By the time we found out that decamethylcobaltocene is, in fact, sufficiently reducing to access the $P_3^BFeN_2^-$ anion after all, that good idea (that we might have a different mechanism at work which might involve the metallocene as more than a reductant) was firmly entrenched. So far we still think we ended up at the right hypothesis for the (initially) wrong reasons.*

4.1 Introduction

The reduction of N_2 to NH_3 is critical for life and is performed on a massive scale both industrially and biologically.[1] The high stability of the N≡N triple bond necessitates catalysts and high-energy reagents/conditions to achieve the desired transformation.[2] Synthetic studies of catalytic N_2-to-NH_3 conversion by model complexes are of interest to constrain hypotheses concerning the mechanism/s of biological (or industrial) N_2-fixation and to map fundamental catalyst design principles for multi-electron reductive transformations.[3,4] Interest in Fe model systems that catalyze N_2-to-NH_3 conversion has grown in part due to the postulate that one or more Fe centers in the FeMo-cofactor of FeMo-nitrogenase may serve as the site of N_2 binding and activation during key bond-breaking and -making steps.[5] Previous examples of synthetic molecular Fe catalysts that mediate N_2-to-NH_3 conversion operate with high driving force, relying on a very strong acid (pK_a ca. 0) and reductant (E° < −3.0 V vs $Fc^{+/0}$).[6,7,8,9] In contrast, several Mo catalysts have been shown to facilitate N_2-to-NH_3 conversion with significantly lower driving force.[10,11,12,13] There is thus interest in exploring the viability of Fe-mediated catalytic N_2-to-NH_3 conversion under less forcing conditions from a practical perspective, and to continue assessing these systems as functional models of biological nitrogenases, in which 8 ATP are consumed per NH_3 formed leading to a driving force of 58 kcal/mol.[2]

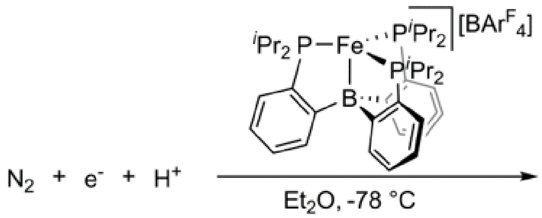

e$^-$ (E^0 vs $Fc^{+/0}$)	H$^+$ (pK_a in THF)	$\Delta\Delta H_f$ (kcal/mol)
Cp^*_2Co (-1.96 V)	[$PhNH_3$][OTf] (7.8)	62
Cp^*_2Co (-1.96 V)	[Ph_2NH_2][OTf] (4.1)	77
KC_8 ($\leq$ -3.0 V)	$HBAr^F_4$ (ca. 0)	$\geq$ 156

Figure 4.1. Summary of conditions used for catalytic N_2-to-NH_3 conversion by $P_3^BFe^+$ highlighting the estimated enthalpic driving force ($\Delta\Delta H_f$).[14,15,16,17,18,19]

Herein we demonstrate that catalytic conversion of N_2 to NH_3 by $P_3^BFe^+$ (P_3^B = tris(*o*-diisopropylphosphinophenyl)borane) can be achieved with a significantly lower driving force by coupling Cp^*_2Co with $[Ph_2NH_2]^+$ or $[PhNH_3]^+$ (Figure 4.1). Such conditions additionally afford unusually high selectivity and catalytic turnover for NH_3.[20] Moreover, we note the use of milder reagents as reductant (E^0; eq 1) and acid (pK_a) engenders a higher effective bond dissociation enthalpy ($BDE_{effective}$; eq 1).15,[21] This may in turn afford access to proton-coupled electron transfer (PCET) pathways (e.g., $FeN_2 + H\cdot \rightarrow FeN_2H$) in addition to electron transfer (ET)/proton transfer (PT) pathways, thus enhancing overall catalytic efficiency. Theoretical considerations, including DFT calculations, and experimental details are discussed that suggest the viability of a decamethylcobaltocene-mediated PCET pathway in this system; by extension we suggest metallocene-mediated (e.g., Cp^*_2Cr) PCET pathways may be operative in previously studied Mo and Fe N_2-fixing systems that use metallocene reductants.10[-]13[,]20

$$BDE_{effective} = 1.37(pK_a) + 23.06(E^0) + C_H \qquad (1)$$

Various observations of P_3^BFe complexes in the presence of acids and reductants suggested that this system might be capable of N_2-to-NH_3 conversion with lower driving force than that originally reported. Accordingly, we had observed that the treatment of $P_3^BFeN_2^-$ with KC_8 and weaker acids ($pK_a > 0$) led to greater than stoichiometric NH_3 formation (e.g., under unoptimized conditions [2,6-dimethylanilinium][OTf] afforded 2.1 equiv NH_3 per Fe).[22] Similarly, the treatment of $P_3^BFeN_2^-$ with $[H(OEt_2)_2][BAr^F_4]$ ($HBAr^F_4$, BAr^F_4 = tetrakis(3,5-bis(trifluoromethyl)phenyl)borate) and weaker reductants led to modest yields of NH_3. For example, under unoptimized conditions we had observed that decamethylcobaltocene (Cp^*_2Co) and $HBAr^F_4$ afforded 0.6 equiv NH_3 per Fe.22[,23] Most recently, an apparent catalytic response was observed during a cyclic voltammetry experiment at the $P_3^BFeN_2^{0/-}$ couple (−2.1 V vs $Fc^{+/0}$) upon addition of excess $HBAr^F_4$ under an N_2 atmosphere. Electrolytic NH_3 generation by $P_3^BFe^+$ was observed at −2.4 V vs $Fc^{+/0}$ in Et_2O,23 and Na/Hg (−2.4 V vs $Fc^{+/0}$ in THF)16 could instead be used for N_2-to-NH_3

conversion catalysis (albeit less selectively and with low turnover). Finally, mixing $P_3^BFe^+$ with Cp^*_2Co in Et_2O at −78 °C under N_2 generates some $P_3^BFeN_2^-$ as observed by X-band EPR and Mössbauer spectroscopy (see SI), suggesting that Cp^*_2Co is in principle a sufficiently strong reductant to trigger catalysis by $P_3^BFe^+$.

4.2 Results and Discussion

Treatment of $P_3^BFe^+$ with Cp^*_2Co and $[Ph_2NH_2][OTf]$, $[Ph_2NH_2][BAr^F_4]$, or $[PhNH_3][OTf]$ in Et_2O at −78 °C under an N_2 atmosphere affords catalytic yields of NH_3 (Table 4.1). Notably, the highest selectivity for NH_3 obtained among this series (72% at standard substrate loading; Entry 1) is significantly improved compared to all previously described (molecular) Fe catalysts for N_2-to-NH_3 conversion.20,[24] Tripling the initial substrate loading (Entry 2) nearly triples the NH_3 production with only modest loss in efficiency for NH_3 (63%). Preliminary attempts to further increase the initial substrate loading have led to substantially decreased efficiency (Entry 3). However, substrate reloading experiments (Entries 4 and 5) maintain greater than 50% efficiency for NH_3 overall; a turnover number for NH_3 generation via two reloadings has been achieved as high as 89 in a single run (84 ± 8; Entry 5). This is an unusually high turnover number for a molecular N_2-to-NH_3 conversion catalyst under any conditions.20,[25]

The use of the more soluble acid $[Ph_2NH_2][BAr^F_4]$ (Entry 6) provides significantly lower, but still catalytic, yields of NH_3. This more soluble acid presumably increases background reactivity with Cp^*_2Co (see SI). Perhaps more significantly, $[PhNH_3][OTf]$ is a considerably weaker acid than $[Ph_2NH_2][OTf]$ (Figure 4.1), but still provides substantial catalytic yields of NH_3 (Entries 7 and 8) and at efficiencies that compare well with those obtained previously using $HBAr^F_4$ and KC_8 despite a difference in driving force of nearly 100 kcal/mol.23

Table 4.1. N_2-to-NH_3 Conversion with P_3^EM Complexes (M = Fe, Co)

	Catalyst	**Cp^*_2Co (equiv)**	**Acid (equiv)**	**Equiv NH_3/Fe**	**% Yield NH_3/e^-**
1	$P_3^BFe^+$	54	108[b]	12.8 ± 0.5	72 ± 3
2	$P_3^BFe^+$	162	322[b]	34 ± 1	63 ± 2
3	$P_3^BFe^+$	322	638[b]	26.7 ± 0.9	25 ± 1
4[a]	$P_3^BFe^+$	[162]x2	[322]x2[b]	56 ± 9	52 ± 9
5[a]	$P_3^BFe^+$	[162]x3	[322]x3[b]	84 ± 8	52 ± 5
6	$P_3^BFe^+$	54	108[c]	8 ± 1	42 ± 6
7	$P_3^BFe^+$	54	108[d]	7 ± 1	38 ± 7
8	$P_3^BFe^+$	162	322[d]	16 ± 3	29 ± 4
9	$P_3^{Si}FeN_2$	54	108[b]	1.2 ± 0.1	6 ± 1
10	$P_3^BCoN_2^-$	54	108[b]	1.1 ± 0.4	6 ± 2
11	$P_3^{Si}CoN_2$	54	108[b]	0 ± 0	0 ± 0

The catalyst, acid, Cp^*_2Co, and Et_2O were sealed in a vessel at −196 °C under an N_2 atmosphere followed by warming to −78 °C and stirring. Yields are reported as an average of at least 2 runs; for individual experiments see SI. [a]For these experiments the reaction was allowed to proceed for 3 hours at −78 °C before cooling to −196 °C and furnished with additional substrate and solvent [b]$[Ph_2NH_2][OTf]$. [c]$[Ph_2NH_2][BAr^F_4]$. [d]$[PhNH_3][OTf]$.

We also screened several related phosphine-ligated Fe–N_2 and Co–N_2 complexes[26,27] under the new standard reaction conditions with $[Ph_2NH_2][OTf]$ and Cp^*_2Co (Entries 9–11) but found that none of these other systems were competent catalysts. While we anticipate other catalyst systems for N_2-to-NH_3 conversion may yet be found that function under the conditions described herein,20 certain features of the P_3^BFe system correlate with unusually productive catalysis.27

Also significant is that when $P_3^BFe^+$ is loaded with 322 equiv [Ph_2NH_2][OTf] and 162 equiv Cp^*_2Co in Et_2O at −78 °C, modest levels of N_2H_4 are detected (< 1 equiv per Fe; see SI).9,20 We had previously reported that catalytic N_2 reduction with KC_8 and $HBAr^F_4$ yielded no detectable hydrazine, but observed that if hydrazine was added at the outset of a catalytic run, it was consumed.6 When 5 equiv of N_2H_4 were added at the beginning of a catalytic run (again with 322 equiv [Ph_2NH_2][OTf] and 162 equiv Cp^*_2Co), only 0.22 equiv of N_2H_4 (4.4% recovery) remained after workup. This result indicates that liberated hydrazine can also be reduced or disproportionated under the present conditions. That N_2H_4 is detected to any extent in the absence of initially added N_2H_4 under these conditions indicates that a late N–N cleavage mechanism to produce NH_3 (e.g., alternating or hybrid cross-over) is accessible.4[,28] A recent report by Ashley and coworkers describes a phosphine-supported Fe system for which catalytic hydrazine formation is kinetically dominant.20 Whether such a pathway is kinetically dominant in this system is as yet unclear.23[,29]

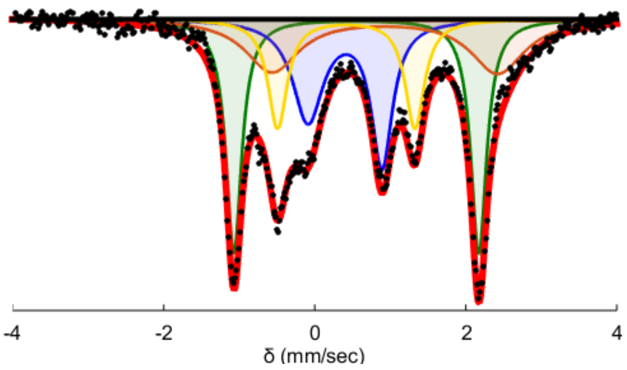

Figure 4.2. Mössbauer spectrum at 80 K with 50 mT applied parallel field of a freeze-quenched catalytic reaction (54 equiv Cp^*_2Co, 108 equiv $[Ph_2NH_2][OTf]$, 1 equiv $P_3^B[^{57}Fe]^+$) after five minutes of reaction time.

The P_3^BFe speciation under turnover conditions was probed via freeze-quench Mössbauer spectroscopy.23 The Mössbauer spectrum of a catalytic reaction mixture after five minutes of reaction time (Figure 4.2) reveals the presence of multiple species featuring well-resolved sets of quadrupole doublets. The spectrum is satisfactorily simulated with $P_3^BFeN_2$ (δ = 0.55 mm/sec, ΔE_Q = 3.24 mm/sec, 32%; Figure 4.2 green), $P_3^BFeN_2^-$ (δ = 0.40 mm/sec, ΔE_Q = 0.98 mm/sec, 26%; Figure 4.2 blue),23,[30] an unknown, likely P_3^B metallated Fe species (δ = 0.42 mm/sec, ΔE_Q = 1.84 mm/sec, 18%; Figure 4.2 yellow), and a final species that is modeled with δ = 0.96 mm/sec and ΔE_Q = 3.10 mm/sec (24%; Figure 4.2 orange). The broad nature of this last signal and its overlap with other features in the spectrum prevents its precise assignment, but its high isomer shift and large quadrupole splitting are suggestive of a tetrahedral, *S* = 2 Fe(II) complex.[31,32] The Mössbauer spectrum of a catalytic reaction mixture after 30 minutes was also analyzed (see SI). The spectrum still shows $P_3^BFeN_2$ (53%), the same unknown P_3^BFe species (18%), and again a tetrahedral, high-spin Fe(II) component (22%). However, $P_3^BFe^+$ is now present (δ = 0.75

mm/sec, ΔE_Q = 2.55 mm/sec, 8%) and $P_3^BFeN_2^-$ is no longer observed. The reloading experiments described above provide strong evidence that "P_3^BFe" species represent an "active catalyst" population; interpretation of the relative speciation via spectroscopy should hence bear on the mechanism of the overall catalysis.

The appearance of a presumed high-spin (S = 2), tetrahedral Fe(II) species during catalysis (ca. 25%) might arise via dechelation of a phosphine arm. This species could represent an off-path state, or a downstream deactivation product. Interestingly, under the present catalytic conditions we do not observe the borohydrido-hydrido species $P_3^B(\mu\text{-}H)Fe(H)(L)$ (L = N_2 or H_2); this species was postulated to be an off-path resting state during N_2-to-NH_3 conversion catalysis using $HBAr^F_4$ and KC_8 and was the major component observed at early times (ca. 60% at 5 min).23 It therefore appears that a larger fraction of the "P_3^BFe" species are in a catalytically on-path state at early reaction times under these new catalytic conditions.

Additionally, the presence of a significant degree of $P_3^BFeN_2^-$ (Figure 4.2) at an early time point is distinct from conditions with $HBAr^F_4$ and KC_8.23 This observation is consistent with the notion that protonation of $P_3^BFeN_2^-$ is slowed under the present conditions, likely as a result of the insolubility of the triflate salt $[Ph_2NH_2][OTf]$ and its attenuated acidity relative to $HBAr^F_4$.17,18,[33] Clearly, differences in the rates of key elementary steps under the new conditions described here may lead to new mechanistic scenarios for N_2-to-NH_3 conversion.

The improved catalytic efficiency at significantly lower driving force warrants additional consideration. When using $HBAr^F_4$ and KC_8 we have previously suggested that protonation of $P_3^BFeN_2^-$, which itself can be generated by reduction of $P_3^BFeN_2$, to produce

$P_3^BFe\text{-}N{=}NH$ is a critical first step; $P_3^BFe\text{-}N{=}NH$ can then be trapped by acid to produce spectroscopically observable $P_3^BFe{=}N\text{-}NH_2^+$.29 These steps, shown in eq 2a-b, represent an ET-PT pathway. A PT-ET pathway, where $P_3^BFeN_2$ is sufficiently basic to be protonated to generate $P_3^BFe\text{-}N{=}NH^+$ as a first step, followed by ET, is also worth considering (eq 3a-b). A direct PCET pathway (eq 4) where H-atom delivery to $P_3^BFeN_2$ occurs, thus obviating the need to access either $P_3^BFeN_2^-$ or $P_3^BFe\text{-}N{=}NH^+$, needs also to be considered.

$$P_3^BFeN_2 + e^- \rightarrow P_3^BFeN_2^- \qquad (2a)$$

$$P_3^BFeN_2^- + H^+ \rightarrow P_3^BFe\text{-}N{=}NH \qquad (2b)$$

$$P_3^BFeN_2 + H^+ \rightarrow P_3^BFe\text{-}N{=}NH^+ \qquad (3a)$$

$$P_3^BFe\text{-}N{=}NH^+ + e^- \rightarrow P_3^BFe\text{-}N{=}NH \qquad (3b)$$

$$P_3^BFeN_2 + H\cdot \rightarrow P_3^BFe\text{-}N{=}NH \qquad (4)$$

Initial PT to $P_3^BFeN_2$ to generate $P_3^BFe\text{-}N{=}NH^+$ (eq 3a) is unlikely under the present conditions due to the high predicted acidity of $P_3^BFe\text{-}N{=}NH^+$ ($pK_a = -3.7$; estimated via DFT; see SI); efficient generation of such a species seems implausible for acids whose pK_a's are calculated at 1.4 ($Ph_2NH_2^+$) and 6.8 ($PhNH_3^+$) in Et_2O (Table 4.2). We note that $[Ph_2NH_2][OTf]$ does not react productively with $P_3^BFeN_2$ at -78 °C in Et_2O, as analyzed by Mössbauer spectroscopy.

Table 4.2. Calculated p*K*a Values and BDEs of Selected Species[a]

Species	**p*K*a**	**BDE**[b]
$Ph_2NH_2^+$	1.4[c]	-
$PhNH_3^+$	6.8	-
Lutidinium	14.5	-
endo-Cp*Co(η^4-C_5Me_5H)$^+$	16.8	31
exo-Cp*Co(η^4-C_5Me_5H)$^+$	16.8	31
endo-Cp*Cr(η^4-C_5Me_5H)$^+$	17.3	37
exo-Cp*Cr(η^4-C_5Me_5H)$^+$	12.1	30
P_3^BFe-N=NH$^+$	-3.7	-
P_3^BFe-N=NH	38.7	35
P_3^BFe=N-NH_2^+	14.4	51
P_3^BFe=N-NH_2	-	47
[HIPTN_3N]Mo-N=NH	-	51

[a]Calculations were performed using the M06-L[34] functional with a def2-TZVP basis set on Fe and a def2-SVP basis set on all other atoms[35] (see SI). [b]In kcal/mol. [c]p*K*a values were calculated in Et_2O and reported relative to $(Et_2O)_2H^+$.

Focusing instead on the PCET pathway (eq 4), the DFT-calculated BDE_{N-H} for P_3^BFe-N=NH (35 kcal/mol; Table 4.2; see SI for details)[36] is larger than the effective BDE21 of either $Cp^*_2Co/Ph_2NH_2^+$ or $Cp^*_2Co/PhNH_3^+$ (25 and 31 kcal/mol, respectively). This suggests that PCET (eq 4) is plausible on thermodynamic grounds. Given that we have employed Cp^*_2Co in this study, and that this and also Cp_2Co and Cp^*_2Cr have been effective in other N_2-fixing molecular catalyst systems,10,11,12,13,20 we have explored via DFT several putative metallocene-derived PCET reagents. Independent studies of H_2 evolution from cobaltocene have invoked a protonated cobaltocene intermediate.[37,38,39] The observation of a background H_2 evolution reaction (HER) when employing metallocene reductants, but in the absence of an N_2-to-NH_3 conversion catalyst, suggests that metallocene protonation is kinetically competent.10,[40] Based on the analysis we describe below, we propose that protonated metallocenes may serve as discrete and highly active H· sources for PCET.

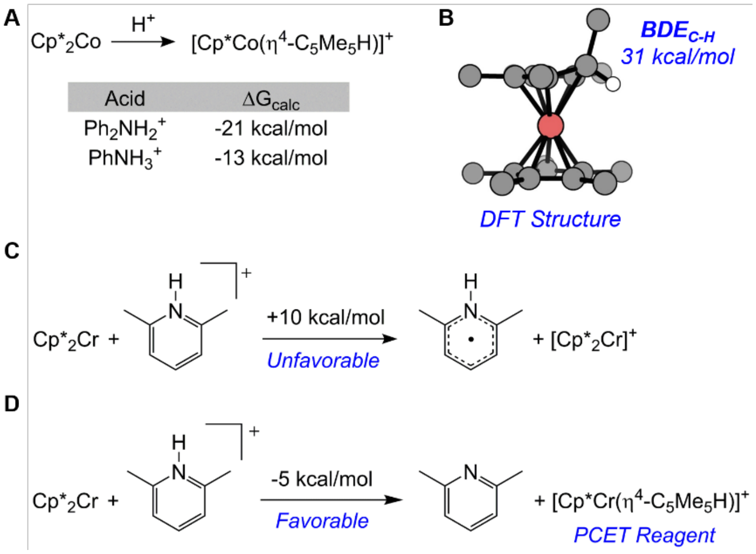

Figure 4.3. (A) Calculated free-energy changes for the protonation of $Cp^*{}_2Co$. (B) DFT optimized structure of *endo*-$Cp^*Co(\eta^4\text{-}C_5Me_5H)^+$ (methyl protons omitted for clarity). (C) The unfavorable reduction of 2,6-lutidinium by $Cp^*{}_2Cr$ with the calculated free energy change. (D) The favorable protonation of $Cp^*{}_2Cr$ by lutidinium with the calculated free energy change.

We find that the formation of *endo*- and *exo*-$Cp^*Co(\eta^4\text{-}C_5Me_5H)^+$ are predicted to be thermodynamically favorable via protonation of $Cp^*{}_2Co$ by either $Ph_2NH_2^+$ or $PhNH_3^+$ (−21 and −13 kcal/mol, respectively; Figure 4.3A).[41,42] We have calculated the $BDE_{C\text{-}H}$'s for both *endo*- and *exo*-$Cp^*Co(\eta^4\text{-}C_5Me_5H)^+$ as 31 kcal/mol (Figure 4.3B; Table 4.2), indicating that they should be among the strongest PCET reagents accessible in this catalyst cocktail. Indeed, they would be among the strongest PCET reagents known.21

We anticipate these species would be extremely unstable in solution and hence difficult to detect in situ, but via trapping in the solid state by rapid precipitation we have isolated a species whose EPR data and chemical behavior are consistent with {Cp*Co(η^4-C_5Me_5H)}{OTf}. Accordingly, slow addition of a toluene solution of $Cp*_2Co$ at -78 °C to triflic acid (HOTf) leads to the instantaneous precipitation of a purple solid that can be isolated at low temperature. The purple solid can be characterized at 77 K by powder EPR spectroscopy via its highly structured signal. By contrast, at this temperature $S = ½$ $Cp*_2Co$ does not display a discernable EPR signal (see SI). The new signal shows strong Co hyperfine coupling and significant g-anisotropy, consistent with a new $S = ½$ cobalt species (Figure 4.4). Furthermore, the resulting EPR signal is slightly perturbed when this purple solid is instead generated from the reaction between deuterated triflic acid (DOTf) and $Cp*_2Co$ (see SI), suggesting that the acidic proton is directly associated with the new Co species and consistent with its assignment as a protonated decamethylcobaltocene species. Close inspection of these spectra indicate they likely represent a mixture of two signals arising from similar Co-containing complexes. This observation is fully consistent with the presence of both *endo*- and *exo*-Cp*Co(η^4-C_5Me_5H)$^+$, as is to be expected given they are predicted to be nearly isoenergetic. Allowing the purple precipitate to warm to room temperature either as a solid or a stirred suspension in toluene leads to the formation of H_2 and $Cp*_2Co^+$ (see SI).

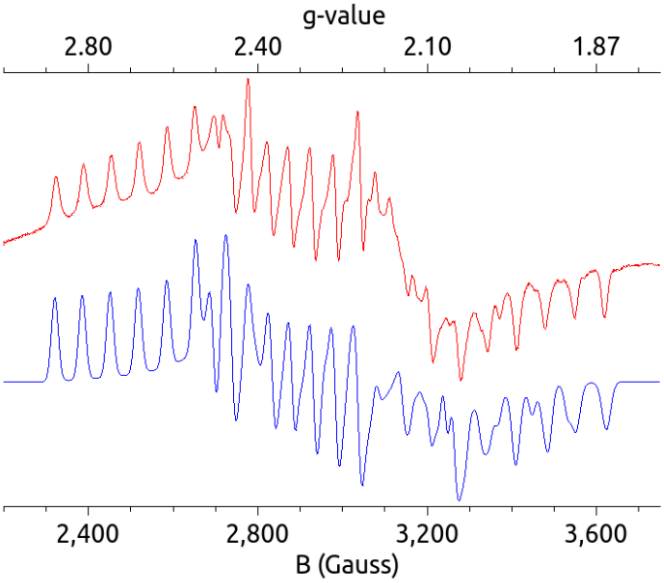

Figure 4.4. X-band 77 K powder EPR spectrum (red) and simulation (blue) of the isolated purple precipitate (assigned as *endo*- and *exo*-Cp*Co(η^4-C_5Me_5H)$^+$) from reaction between Cp^*_2Co and HOTf at -78 °C (see SI for simulation parameters).

To better understand the potential role of PCET in N_2-to-NH_3 conversion catalysis by P_3^BFe, we have additionally calculated the N–H bond strengths (Table 4.2) of several early stage candidate intermediates, including the aforementioned P_3^BFe-N=NH (35 kcal/mol), P_3^BFe=N-NH_2^+ (51 kcal/mol), and P_3^BFe=N-NH_2 (47 kcal/mol). We conclude that PCET from Cp*Co(η^4-C_5Me_5H)$^+$ to generate intermediates of these types is thermodynamically favorable in each case.[43] To generate the first and most challenging intermediate (eq 5), the enthalpic driving force for PCET is estimated at ~4 kcal/mol ($\Delta G_{calc} = -9$ kcal/mol). This driving force, and hence the plausibility of PCET steps, increases sharply as further downstream Fe-N_xH_y intermediates are considered.[44,45,46,47]

$$P_3^BFeN_2 + Cp^*Co(\eta^4\text{-}C_5Me_5H)^+ \rightarrow P_3^BFe\text{-}N{=}NH + Cp^*_2Co^+ \quad (5)$$

Given the prevalence of metallocene reductants in N_2-to-NH_3 (or -N_2H_4) conversion,10,11,12,13,20 especially for the well-studied Mo catalyst systems, it is worth considering metallocene-mediated PCET more generally. For instance, a role for ET/PT steps (or conversely PT/ET) in N_2-to-NH_3 conversion catalyzed by [HIPTN$_3$N]Mo (HIPTN$_3$N = $[(3,5\text{-}(2,4,6\text{-}{}^iPr_3C_6H_2)_2C_6H_3NCH_2CH_2)_3N]^{3-}$, a bulky triamidoamine ligand) has been frequently posited.[48,49,50,51,52] But PCET steps may play a critical role, too. In the latter context, we note reports from Schrock and coworkers that have shown both acid and reductant are required to observe productive reactivity with [HIPTN$_3$N]MoN$_2$. These observations are consistent with PCET to generate [HIPTN$_3$N]Mo-N=NH.52 A PCET scenario has been discussed in this general context of N_2-to-NH_3 conversion, where a lutidinyl radical intermediate formed via ET from Cp*$_2$Cr has been suggested as a PCET reagent that can be generated in situ.40,[53] However, our own calculations predict that the lutidinyl radical should not be accessible with Cp*$_2$Cr as the reductant (ΔG_{calc} = +10 kcal/mol; Figure 4.3C).[54,55,56] We instead propose protonation of Cp*$_2$Cr by the lutidinium acid as more plausible (ΔG_{calc} = −5.3 kcal/mol; Figure 4.3D) to generate a highly reactive decamethylchromocene-derived PCET reagent.

While N–H bond strengths have not been experimentally determined for the [HIPTN$_3$N]Mo-system, using available published data we deduce the N–H bond of [HIPTN$_3$N]Mo-N=NH to be ca. 49 kcal/mol and we calculate it via DFT (truncated HIPTN$_3$N; see SI) as 51 kcal/mol.[57] The BDE$_{N\text{-}H}$ for this Mo diazenido species is hence much larger than we predict for P_3^BFe-N=NH (35 kcal/mol), perhaps accounting for its higher stability.52 A PCET reaction between *endo*-Cp*Cr(η^4-C_5Me_5H)$^+$ (BDE_{calc} = 37 kcal/mol) and [HIPTN_3N]MoN_2 to generate [HIPTN_3N]Mo-N=NH and Cp*$_2$Cr$^+$ would be highly exergonic. Furthermore, we predict a similarly weak $BDE_{C\text{-}H}$ for Cp-protonated cobaltocene, CpCo(η^4-C_5H_6)$^+$ (BDE_{calc} = 35 kcal/mol). These considerations are consistent with the reported rapid formation of [HIPTN_3N]Mo-N=NH using either Cp*$_2$Cr or Cp_2Co in the presence of lutidinium acid.[58]

4.3 Conclusion

To close, we have demonstrated catalytic N_2-to-NH_3 conversion by $P_3^BFe^+$ at a much lower driving force (nearly 100 kcal/mol) than originally reported via combination of a weaker reductant (Cp*$_2$Co) and acid ([Ph_2NH_2][OTf] or [Ph_3NH][OTf]). Significantly improved efficiency for NH_3 formation is observed (up to 72% at standard substrate loading), and by reloading additional substrate at low temperature a turnover number that is unusually high for a synthetic molecular catalyst (84 ± 8 equiv NH_3 per Fe) has been achieved. Freeze-quench Mössbauer spectroscopy under turnover conditions reveals differences in the speciation of P_3^BFe compared to previous studies with $HBAr^F_4$ and KC_8, suggesting changes in the rates of key elementary steps. Using DFT calculations we have considered the viability of a decamethylcobaltocene-mediated PCET pathway as an additional or alternative scenario to previously formulated ET-PT and PT-ET pathways. Based on our calculations, we propose that protonated metallocenes should serve as discrete, very reactive PCET reagents in N_2-to-NH_3 conversion catalysis. Furthermore, we present preliminary experimental data that suggest protonated decamethylcobaltocene can be accessed synthetically and that such a species may be a potent PCET reagent. Indeed, the achievement of high efficiency for N_2-to-NH_3 conversion by both P_3^BFe and various Mo catalysts that benefit from metallocene reductants raises the intriguing possibility that metallocene-based PCET reactivity is a potentially widespread and overlooked mechanism. Efforts are underway to experimentally probe such pathways.

4.4 REFERENCES

[1] Smil, V. *Enriching the Earth.* Cambridge: MIT Press, 2001.

[2] Ham, C. J. M. van der; Koper, M. T. M.; Hetterscheid, D. G. H. Challenges in Reduction of Dinitrogen by Proton and Electron Transfer. *Chem. Soc. Rev.* **2014**, *43*, 5183–5191.

[3] Shaver, M. P.; Fryzuk, M. D. Activation of Molecular Nitrogen: Coordination, Cleavage and Functionalization of N2 Mediated By Metal Complexes. *Adv. Synth. Catal.* **2003**, *345*, 1061–1076.

[4] MacLeod, K. C.; Holland, P. L. Recent Developments in the Homogeneous Reduction of Dinitrogen by Molybdenum and Iron. *Nat Chem* **2013**, *5*, 559–565.

[5] Hoffman, B. M.; Lukoyanov, D.; Yang, Z.-Y.; Dean, D. R.; Seefeldt, L. C. Mechanism of Nitrogen Fixation by Nitrogenase: The Next Stage. *Chem. Rev.* **2014**, *114*, 4041–4062.

[6] Anderson, J. S.; Rittle, J.; Peters, J. C. Catalytic Conversion of Nitrogen to Ammonia by an Iron Model Complex. *Nature* **2013**, *501*, 84–87.

[7] Creutz, S. E.; Peters, J. C. Catalytic Reduction of N2 to NH3 by an Fe–N2 Complex Featuring a C-Atom Anchor. *J. Am. Chem. Soc.* **2014**, *136*, 1105–1115.

[8] Ung, G.; Peters, J. C. Low-Temperature N_2 Binding to Two-Coordinate L_2Fe^0 Enables Reductive Trapping of $L_2FeN_2^-$ and NH_3 Generation. *Angew. Chem. Int. Ed.* **2015**, *54*, 532–535.

[9] Kuriyama, S.; Arashiba, K.; Nakajima, K.; Matsuo, Y.; Tanaka, H.; Ishii, K.; Yoshizawa, K.; Nishibayashi, Y. Catalytic Transformation of Dinitrogen into Ammonia and Hydrazine by Iron-Dinitrogen Complexes Bearing Pincer Ligand. *Nat. Commun.* **2016**, *7*, 12181.

[10] Yandulov, D. V.; Schrock, R. R. Catalytic Reduction of Dinitrogen to Ammonia at a Single Molybdenum Center. *Science* **2003**, *301*, 76–78.

[11] Arashiba, K.; Miyake, Y.; Nishibayashi, Y. A Molybdenum Complex Bearing PNP-Type Pincer Ligands Leads to the Catalytic Reduction of Dinitrogen into Ammonia. *Nat. Chem.* **2011**, *3*, 120–125.

[12] Kuriyama, S.; Arashiba, K.; Nakajima, K.; Tanaka, H.; Kamaru, N.; Yoshizawa, K.; Nishibayashi, Y. Catalytic Formation of Ammonia from Molecular Dinitrogen by Use of Dinitrogen-Bridged Dimolybdenum–Dinitrogen Complexes Bearing PNP-Pincer Ligands: Remarkable Effect of Substituent at PNP-Pincer Ligand. *J. Am. Chem. Soc.* **2014**, *136*, 9719–9731.

[13] Arashiba, K.; Kinoshita, E.; Kuriyama, S.; Eizawa, A.; Nakajima, K.; Tanaka, H.; Yoshizawa, K.; Nishibayashi, Y. Catalytic Reduction of Dinitrogen to Ammonia by Use of Molybdenum–Nitride Complexes Bearing a Tridentate Triphosphine as Catalysts. *J. Am. Chem. Soc.* **2015**, *137*, 5666–5669.

[14] The enthalpic driving force ($\Delta\Delta H_f$) has been estimated here by taking $3*(BDE_{H\cdot} - BDE_{effective})$, where BDE is bond dissociation enthalpy. This allows for an evaluation of the driving force for a given reaction with respect to that for a hypothetical N_2-to-NH_3 conversion catalyst that uses H_2 as the proton and electron source. This is achieved by using Bordwell's equation (with the assumption that $S(X^\cdot) = S(XH)$; see SI) and literature values for p*K*a, redox potential, the enthalpy of reaction for $H^+ + e^- \rightarrow H^\cdot$ ($C_H = 66$ kcal/mol in THF), and the energy of $H^\cdot$ in THF (52 kcal/mol).

[15] Bordwell, F. G.; Cheng, J. P.; Harrelson, J. A. Homolytic Bond Dissociation Energies in Solution from Equilibrium Acidity and Electrochemical Data. *J. Am. Chem. Soc.* **1988**, *110*, 1229–1231.

[16] Connelly, N. G.; Geiger, W. E. Chemical Redox Agents for Organometallic Chemistry. *Chem. Rev.* **1996**, *96*, 877–910.

[17] Garido, G.; Rosés, M.; Ràfols, C.; Bosch, E. Acidity of Several Anilinium Derivatives in Pure Tetrahydrofuran. *J. Sol. Chem.* **2008**, *37,* 689-700.

[18] Kaljurand, I.; Kütt, A.; Sooväli, L.; Rodima, T.; Mäemets, V.; Leito, I.; Koppel, I. A. Extension of the Self-Consistent Spectrophotometric Basicity Scale in Acetonitrile to a Full Span of 28 pKa Units: Unification of Different Basicity Scales. *J. Org. Chem.* **2005**, *70*, 1019–1028.

[19] Cappellani, E. P.; Drouin, S. D.; Jia, G.; Maltby, P. A.; Morris, R. H.; Schweitzer, C. T. Effect of the Ligand and Metal on the pK_a Values of the Dihydrogen Ligand in the Series of Complexes $[M(H_2)H(L)_2]^+$, M = Fe, Ru, Os, Containing Isosteric Ditertiaryphosphine Ligands, L. *J. Am. Chem. Soc.* **1994**, *116*, 3375–3388.

[20] While initiating our studies we became aware of a phosphine-supported Fe system that catalyzes N_2-to-N_2H_4 conversion using Cp^*_2Co and $[Ph_2NH_2][OTf]$ with efficiency as high as 72% for e^- delivery to N_2: Hill, P. J.; Doyle, L. R.; Crawford, A. D.; Myers, W. K.; Ashley, A. E. Selective Catalytic Reduction of N2 to N2H4 by a Simple Fe Complex. *J. Am. Chem. Soc.* **2016**, *138*, 13521–13524.

[21] Warren, J. J.; Tronic, T. A.; Mayer, J. M. Thermochemistry of Proton-Coupled Electron Transfer Reagents and its Implications. *Chem. Rev.* **2010**, *110*, 6961-7001.

[22] Anderson, J. S. *Catalytic conversion of nitrogen to ammonia by an iron model complex. Ph.D. Thesis, California Institute of Technology, September 2013.*

[23] Del Castillo, T. J.; Thompson, N. B.; Peters, J. C. A Synthetic Single-Site Fe Nitrogenase: High Turnover, Freeze-Quench ^{57}Fe Mössbauer Data, and a Hydride Resting State. *J. Am. Chem. Soc.* **2016**, *138*, 5341–5350.

[24] Previously reported molecular Fe catalysts for N_2-to-NH_3 conversion utilize KC_8 and $HBAr^F_4$ and achieve NH_3 selectivities ≤ 45% with respect to their limiting reagent (see refs 6-9) at a similar reductant loading. Lower selectivities are observed with higher loading (see refs 6 and 23).

[25] In catalytic runs performed with labeled $[Ph_2{}^{15}NH_2][OTf]$ under an atmosphere of natural abundance $^{14}N_2$ the production of exclusively $^{14}NH_3$ is observed, demonstrating that the NH_3 formed during catalysis is derived from N_2 and not degradation of the acid (see SI).

[26] Whited, M. T.; Mankad, N. P.; Lee, Y.; Oblad, P. F.; Peters, J. C. Dinitrogen Complexes Supported by Tris(phosphino)silyl Ligands. *Inorg. Chem.* **2009**, *48*, 2507–2517.

[27] Del Castillo, T. J.; Thompson, N. B.; Suess, D. L. M.; Ung, G.; Peters, J. C. Evaluating Molecular Cobalt Complexes for the Conversion of $\mathrm{N_2}$ to $\mathrm{NH_3}$. *Inorg. Chem.* **2015**, *54*, 9256–9262.

[28] Rittle, J.; Peters, J. C. An Fe-$\mathrm{N_2}$ Complex That Generates Hydrazine and Ammonia via $\mathrm{Fe{=}NNH_2}$: Demonstrating a Hybrid Distal-to-Alternating Pathway for $\mathrm{N_2}$ Reduction. *J. Am. Chem. Soc.* **2016**, *138*, 4243–4248.

[29] Anderson, J. S.; Cutsail, G. E.; Rittle, J.; Connor, B. A.; Gunderson, W. A.; Zhang, L.; Hoffman, B. M.; Peters, J. C. Characterization of an $\mathrm{Fe{\equiv}N{-}NH_2}$ Intermediate Relevant to Catalytic $\mathrm{N_2}$ Reduction to $\mathrm{NH_3}$. *J. Am. Chem. Soc.* **2015**, *137*, 7803–7809.

[30] The presence of $\mathrm{P_3^BFeN_2^-}$ was confirmed by freeze-quench EPR spectroscopy experiments (see SI). The asymmetry observed in the Mössbauer lineshapes is characteristic of this species. A redox equilibrium between $\mathrm{P_3^BFeN_2^{0/-}}$ and $\mathrm{Cp^*{}_2Co^{+/0}}$ is also observed in the reaction of $\mathrm{P_3^BFe^+}$ with excess $\mathrm{Cp^*{}_2Co}$ in the absence of acid (see SI).

[31] The distinct properties of tetrahedral, high spin Fe(II) leads to high isomer shifts (0.9-1.3) and large quadrupole splittings (> 2.5) that are characteristic of these types of species: E. Münck, in *Physical Methods in Bioinorganic Chemistry: Spectroscopy and Magnetism* (Ed.: L. Que Jr.), University Science Books, Sausalito, CA, **2000**, pp. 287-320.

[32] Daifuku, S. L.; Kneebone, J. L.; Snyder, B. E. R.; Neidig, M. L. Iron(II) Active Species in Iron–Bisphosphine Catalyzed Kumada and Suzuki–Miyaura Cross-Couplings of Phenyl Nucleophiles and Secondary Alkyl Halides. *J. Am. Chem. Soc.* **2015**, *137*, 11432–11444.

[33] Hamashima, Y.; Somei, H.; Shimura, Y.; Tamura, T.; Sodeoka, M. Amine-Salt-Controlled, Catalytic Asymmetric Conjugate Addition of Various Amines and Asymmetric Protonation. *Org. Lett.* **2004**, *6*, 1861–1864.

[34] Zhao, Y.; Truhlar, D. G. A New Local Density Functional for Main-Group Thermochemistry, Transition Metal Bonding, Thermochemical Kinetics, and Noncovalent Interactions. *J. Chem, Phys.* **2006**, *125*, 194101: 1-18.

[35] Weigend, F.; Ahlrichs, R. Balanced Basis Sets of Split Valence, Triple Zeta Valence and Quadruple Zeta Valence Quality for H to Rn: Design and Assessment of Accuracy. *Phys. Chem. Chem. Phys.* **2005**, *7*, 3297–3305.

[36] Experimental BDE$_{N\text{-}H}$'s for related species (P_3^{Si}Fe-C=NH$^+$, P_3^{Si}Fe-C=NH, P_3^{Si}Fe-C=N(Me)H$^+$, P_3^{Si}Fe-C=N(Me)H, and P_3^{Si}Fe-N=N(Me)H$^+$) have been measured and are in good agreement with the BDE$_{N\text{-}H}$ values calculated using the DFT methods described in this work (see SI for full details): Rittle, J.; Peters, J. C. *manuscript submitted for publication.*

[37] Koelle, U.; Infelta, P. P.; Graetzel, M. Kinetics and Mechanism of the Reduction of Protons to Hydrogen by Cobaltocene. *Inorg. Chem.* **1988**, *27*, 879–883.

[38] Pitman, C. L.; Finster, O. N. L.; Miller, A. J. M. Cyclopentadiene-Mediated Hydride Transfer from Rhodium Complexes. *Chem. Commun.* **2016**, *52*, 9105–9108.

[39] Quintana, L. M. A.; Johnson, S. I.; Corona, S. L.; Villatoro, W.; Goddard, W. A.; Takase, M. K.; VanderVelde, D. G.; Winkler, J. R.; Gray, H. B.; Blakemore, J. D. Proton–hydride Tautomerism in Hydrogen Evolution Catalysis. *PNAS* **2016**, *113*, 6409–6414.

[40] Munisamy, T.; Schrock, R. R. An Electrochemical Investigation of Intermediates and Processes Involved in the Catalytic Reduction of Dinitrogen by [HIPTN$_3$N]Mo (HIPTN$_3$N = (3,5-(2,4,6-I-Pr$_3$C$_6$H$_2$)$_2$C$_6$H$_3$NCH$_2$CH$_2$)$_3$N). *Dalton Trans.* **2011**, *41*, 130–137.

[41] Efforts to instead optimize a metal hydride species, [Cp*$_2$Co-H]$^+$, led to hydride transfer to the ring system. Nevertheless, reactive transition metal hydride radical cations are also known to exhibit PCET behavior.

[42] Hu, Y.; Shaw, A. P.; Estes, D. P.; Norton, J. R. Transition-Metal Hydride Radical Cations. *Chem. Rev.* **2016**, *116*, 8427–8462

[43] The dissolution equilibria and kinetics of the insoluble reagents used complicate analysis of the kinetics of individual ET, PT, and PCET steps. However, the low activation barriers ($G^{\ddagger} < 9$ kcal/mol) calculated for all proposed PCET reactions are consistent with these reactions being kinetically accessible (see SI for full details).

[44] Studies have shown that the Marcus cross-relation holds quite well for many PCET reactions. This is indicative of a substantial correlation between thermodynamic driving force and reaction kinetics; it is, however, unclear whether the proposed reactivity would demonstrate such behavior.

[45] Roth, J. P.; Yoder, J. C.; Won, T.-J.; Mayer, J. M. Application of the Marcus Cross Relation to Hydrogen Atom Transfer Reactions. *Science* **2001**, *294*, 2524–2526.

[46] Mayer, J. M.; Rhile, I. J. Thermodynamics and Kinetics of Proton-Coupled Electron Transfer: Stepwise vs. Concerted Pathways. *Biochimica et Biophysica Acta (BBA) - Bioenergetics* **2004**, *1655*, 51–58.

[47] Hammes-Schiffer, S. Theoretical Perspectives on Proton-Coupled Electron Transfer Reactions. *Acc. Chem. Res.* **2001**, *34*, 273-281.

[48] Studt, F.; Tuczek, F. Energetics and Mechanism of a Room-Temperature Catalytic Process for Ammonia Synthesis (Schrock Cycle): Comparison with Biological Nitrogen Fixation. *Angew. Chem. Int. Ed.* **2005**, *44*, 5639-5642.

[49] Reiher, M.; Le Guennic, B.; Kirchner, B. Theoretical Study of Catalytic Dinitrogen Reduction under Mild Conditions. *Inorg. Chem.* **2005**, *44*, 9640–9642.

[50] Studt, F.; Tuczek, F. Theoretical, Spectroscopic, and Mechanistic Studies on Transition-Metal Dinitrogen Complexes: Implications to Reactivity and Relevance to the Nitrogenase Problem. *J. Comput. Chem.* **2006**, *27*, 1278–1291.

[51] Thimm, W.; Gradert, C.; Broda, H.; Wennmohs, F.; Neese, F.; Tuczek, F. Free Reaction Enthalpy Profile of the Schrock Cycle Derived from Density Functional Theory Calculations on the Full [MoHIPTN_3N] Catalyst. *Inorg. Chem.* **2015**, *54*, 9248–9255.

[52] Yandulov, D. V.; Schrock, R. R. Studies Relevant to Catalytic Reduction of Dinitrogen to Ammonia by Molybdenum Triamidoamine Complexes. *Inorg. Chem.* **2005**, *44*, 1103–1117.

[53] Pappas, I.; Chirik, P. J. Catalytic Proton Coupled Electron Transfer from Metal Hydrides to Titanocene Amides, Hydrazides and Imides: Determination of Thermodynamic Parameters Relevant to Nitrogen Fixation. *J. Am. Chem. Soc.* **2016**, *138*, 13379–13389.

[54] Although our calculations for a hypothetical lutidinyl radical predict a weak N–H bond ($BDE_{N\text{-}H}$ ~ 35 kcal/mol), the oxidation potential of this species is calculated to be −1.89 V vs $Fc^{+/0}$ in THF (see SI). Experimental determination of this reduction potential for calibration has been contentious; however, our calculated reduction potential is similar to that previously calculated for pyridinium in aqueous media (−1.37 V vs SCE).

[55] Yan, Y.; Zeitler, E. L.; Gu, J.; Hu, Y.; Bocarsly, A. B. Electrochemistry of Aqueous Pyridinium: Exploration of a Key Aspect of Electrocatalytic Reduction of CO_2 to Methanol. *J. Am. Chem. Soc.* **2013**, *135*, 14020–14023.

[56] Keith, J. A.; Carter, E. A. Theoretical Insights into Pyridinium-Based Photoelectrocatalytic Reduction of CO_2. *J. Am. Chem. Soc.* **2012**, *134*, 7580–7583.

[57] It has been reported that [HIPTN_3N]MoN_2^-/[HIPTN_3N]Mo-N=NH is in equilibrium with DBU/$DBUH^+$ (DBU = 1,8-diazabicyclo[5.4.0]undec-7-ene; pK_a = 18.5 in THF; see refs 7c-d). Taken with the reported reduction potential of [HIPTN_3N]MoN_2 ($E_{1/2}$ = −1.81 V vs $Fc^{+/0}$ in THF, see ref 52), the experimental BDE can be approximated with the Bordwell equation and the enthalpy of reaction for $H^+ + e^- \rightarrow H^\cdot$ (see refs 15 and 19).

[58] In addition to lutidinium salts, $[Et_3NH][OTf]$ has been shown to affect the formation of $[HIPTN_3N]Mo\text{-}N{=}NH$ from $[HIPTN_3N]MoN_2$ in the presence of metallocene reductants (see ref 52).